J Am Oil Chem Soc (2008) 85:501–511
DOI 10.1007/s11746-008-1219-9

ORIGINAL PAPER

Influence of Polymorphic Transformations on Gelation of Tripalmitin Solid Lipid Nanoparticle Suspensions

T. Helgason · T. S. Awad · K. Kristbergsson · D. J. McClements · J. Weiss

Received: 18 November 2007 / Revised: 1 February 2008 / Accepted: 19 February 2008 / Published online: 7 March 2008
© AOCS 2008

Abstract Solid lipid nanoparticle (SLN) suspensions, which consist of submicron-sized crystalline lipid particles dispersed within an aqueous medium, can be used to encapsulate, protect and deliver lipophilic functional components. Nevertheless, SLN suspensions are susceptible to particle aggregation and gelation during their preparation and storage, which potentially limits their industrial utilization. In this study, we examined the aggregation and gelation behavior of SLN suspensions composed of 10 wt% tripalmitin particles ($r < 150$ nm) stabilized by 1.5% Tween 20. The tripalmitin and aqueous surfactant solution were homogenized above the lipid melting temperature and cooled under controlled conditions to initiate SLN formation. The aggregation and gelation of SLN suspensions during storage was then examined by shear rheometry, differential scanning calorimetry (DSC), light scattering and microscopy. Rheology measurements indicated that gelation times decreased with increasing storage temperature, e.g., samples formed weak gels after 62, 23, and 10 min at 1, 5, and 10 °C, respectively. DSC revealed increasingly rapid α- to β-polymorphic transformations in SLN dispersions stored at 1, 5, and 10 °C, respectively. We propose that the observed aggregation and gelation of SLN suspensions are associated with a change in the shape of the nanoparticles from spherical (α-form) to non-spherical (β-form) when they undergo the polymorphic transition. When they change shape there is no longer sufficient surfactant present to completely cover the lipid phase, which promotes particle aggregation through hydrophobic attraction. Our results have important implications for the design and fabrication of stable SLN suspensions.

Keywords Solid lipid nanoparticles · Encapsulation · Polymorphic transformations

T. Helgason · K. Kristbergsson
Department of Food Science, University of Iceland, Hjardarhagi 2-6, 107 Reykjavik, Iceland

T. Helgason · T. S. Awad · D. J. McClements · J. Weiss (✉)
Department of Food Science, University of Massachusetts, 100 Holdsworth Way, Amherst, MA 01003, USA
e-mail: jweiss1@foodsci.umass.edu

Introduction

Solid-lipid nanoparticles are colloidal carrier systems that have been developed to encapsulate, protect and deliver lipophilic functional components, such as bioactive lipids and drugs [1–4]. They are manufactured by homogenizing a premix of liquid lipid phase (carrier lipid melt plus functional ingredients) and an aqueous surfactant solution at temperatures above the melting temperature of the carrier lipid to produce a fine oil-in-water emulsion. This emulsion is then cooled to below the crystallization temperature of the carrier lipid leading to the formation of solid particles [5]. The use of solid lipids instead of liquid lipids has been shown to increase control over the release kinetics of the encapsulated compounds and improve the stability of incorporated chemically sensitive drugs [6–8]. This is because firstly the mobility of reactive agents in a solid matrix is lower than in a liquid matrix and oxidative reactions may therefore be reduced. Secondly, microphase separations of drugs and carrier lipid in individual liquid particles resulting in the accumulation of the drug at the surface of the lipid particles where oxidation is prevalent may be prevented [9–15].

Solid-lipid nanoparticles are being widely used in the pharmaceutical industry, but they also have great potential for the encapsulation, protection and delivery of bioactive

food components. For food applications, SLN must be fabricated entirely from generally recognized as safe (GRAS) ingredients using production processes that are economic and allow production of large quantities. Previously, it has been reported that SLN suspensions are highly unstable to aggregation and gelation under certain conditions [16–20]. If SLN are going to be utilized by the food industry it is important to ascertain the origin of this phenomenon, the factors that affect it, and develop effective strategies to prevent it.

Based on previous studies reported in the literature, we hypothesize that the morphology and composition of crystallized lipids may play a key role in the instability in SLN suspensions [21, 22]. Triacylglycerols are known to crystallize upon cooling into different polymorphic forms that vary in their unit cell structures due to differences in molecular conformation and packing [23]. Saturated triacylglycerols may crystallize into three major polymorphic forms (α, β' and β), with the activation energy, thermodynamic stability, packing density, ordering and melting point increasing from the α to β' to β form [23–25].

In this study, we examined the impact of storage conditions on the stability and crystal structure of suspensions of SLN composed of a model triacylglycerol (tripalmitin) stabilized by a food-grade nonionic surfactant (Tween 20).

Materials

Tripalmitin (#92903) was purchased from Fluka (Buchs, Switzerland). Sodium phosphate monobasic (#7558-80-7) and sodium phosphate dibasic (#7558-79-4) were purchased form Fisher Scientific (St Clair Shores, MI, USA). Sodium azide (S2002) and polyethylene glycol sorbitan monolaurate (Tween 20) (374348) were purchased from Sigma-Aldrich Chemical Company (St Louis, MO, USA).

Methods

Solution Preparation

A buffer solution (pH 7) was prepared by dissolving 4 mM sodium phosphate (monobasic) and 6 mM sodium phosphate (dibasic) in distilled water. An aqueous surfactant solution was prepared by dispersing 1.5% (w/w) Tween 20 and 0.02% (w/w) sodium azide (to prevent microbial growth) in phosphate buffer.

Preparation of SLN

Solid-lipid nanoparticles were prepared using a hot high-pressure homogenization method. The lipid phase, tripalmitin, was fully melted in a water bath set at 80 ± 0.5 °C and 10% w/w mixed with 90% w/w surfactant/buffer solution held at the same temperature. The resulting system was mixed for 2 min with a hand-held high-speed blender (model SDT-1810, EN shaft, Tekmar Co., Cincinnati, OH, USA) to form a coarse hot emulsion premix. The hot emulsion premix was then homogenized ten times at 9,000 bars using a thermostatted microfluidizer (Microfluidics, Newton MA, USA) at 75–80 °C to prevent solidification during the homogenization procedure. The ten passes through the microfluidizer took approximately 10 min. The fine dispersed emulsion with a hydrodynamic radius of 146.6 ± 0.9 nm and a polydispersity index of 0.070 ± 0.015 was sealed and placed in a temperature-controlled incubator at 37 °C. In agreement with previous studies our preliminary experiments showed that significant supercooling to below 20 °C was required to induce crystallization [26]. As a result, emulsions maintained at 37 °C consisted of liquid tripalmitin.

Particle Size Determination

Particle size measurements were performed by photon correlation spectroscopy (PCS) (Nano ZS, Malvern Instruments, Malvern, UK). Samples were diluted 1:100 using a phosphate buffer solution to prevent multiple scattering effects. The PCS instrument reports the mean hydrodynamic radius (r) of the particle population and the polydispersity index (PI) ranging from 0 (monodisperse) to 0.50 (very broad distribution). Mean particle size was measured at 37 °C for liquid emulsions using a refractive index of 1.43 (for liquid lipid) and at 5 and 10 °C for SLN using a refractive index of 1.54 (for solid lipid) [27].

Differential scanning calorimetry

The physical state of the emulsified tripalmitin (e.g., solid or liquid) and crystal structures of solid lipids were determined by differential scanning calorimetry (DSC; Q1000, TA Instruments, New Castle, DE, USA). Emulsions (8–10 mg) were placed in aluminum pans and hermetically sealed. Empty pans were used as a reference for the emulsion samples. For the investigation of bulk material, about 1–2 mg of sample was used. The pans were placed in the DSC and cooled down to 1, 5 and 10 °C at 5 °C/min (approximately the same cooling rate as in the ice bath) to induce formation of SLN. After storage for 0, 5, 10, 15, 30, 60, and 120 min the pans were heated to 75 °C at 10 °C/min. Finally the samples were cooled back to 10 °C at 10 °C/min to observe crystallization of re-melted lipid.

Rheometry

Storage modulus (G′) and loss modulus (G″) of SLN suspensions undergoing a sol to gel transition was measured with an oscillatory rheometer (Physica MCR 300, Anton Paar, Graz, Austria) using a cone and plate measurement system (diameter 49.94 mm, angle 2°) thermostatted by a Peltier system. The cone was positioned 50 μm above the plate to avoid effects from single particles. Initially, the linear viscoelastic region was determined by conducting a strain sweep at an oscillation frequency of 1 Hz. The strain sweep indicated that G′ and G″ of gelled samples did not decrease at strains less than 0.8% and consequently all gelation experiments were conducted at a constant strain of 0.1% and frequency of 1 Hz. To determine the influence of holding temperature on the rheological properties of suspensions, samples were first cooled in an ice bath under stirring (300 rpm) and then loaded into the rheometer thermostatted to 1, 5, and 10 °C, and loss and storage modulus measured as a function of time.

Microscopy

The microstructures of emulsions and SLN after cooling were assessed by optical microscopy. A drop of sample was placed on a microscope slide and covered by a cover slip, and then the microstructure was determined using optical microscopy (Nikon microscope Eclipse E400, Nikon Corporation, Japan). Images were acquired using a CCD camera (CCD-300-RC, DAGE-MTI, Michigan City, IN, USA) connected to digital image processing software (Micro Video Instruments, Inc., Avon, MA, USA) installed on a computer. A heating/cooling stage unit (LTS120, Linkam Scientific Instruments, Ltd, England) with a temperature accuracy of ±0.1 °C was used to cool/heat the sample. The heating/cooling stage was equipped with a thermo-electric Peltier unit controlled by a PE 94 controller in combination with an ECP water circulator. Heating and cooling profiles were programmed using the Linksys 32 software.

Stability Assessment of Gelled Sample After Melting

To investigate the stability of gelled SLN upon reheating, 10 ml of the tripalmitin emulsion at 37 °C was placed in a test tube and cooled down to 5 °C and samples withdrawn after 5 and 60 min. Photographic images of the test tubes were taken using a digital camera (PowerShot SD700 IS, Canon, Tokyo, Japan). Samples were then heated to 75 °C to melt the crystallized lipid and photographic images were again taken to evaluate whether coalescence and oiling off had occurred. Additionally, microscopic images were taken for the gelled, un-gelled and melted systems, which were similarly treated inside the Linkam heating/cooling stage. Particle size distribution of samples subjected to heating was measured using a static light scattering technique (Mastersizer X, Malvern Instruments Ltd., Malvern, UK). This instrument determines the particle size distribution of dispersions by measuring the intensity of scattered light as a function of scattering angle and fitting the light scattering data to a theoretical light scattering model (e.g., Mie theory) [26].

Assessment of Effect of Surfactant Concentration on Stability of Samples

The influence of excess surfactant in the aqueous phase of the SLN suspensions on their stability to aggregation and gelation was examined by taking aliquots of warm SLN suspensions (37 °C) that had been freshly homogenized and mixing them with a surplus of Tween 20 (1, 2, 5 wt%) prior to cooling to obtain suspensions that had overall surfactant concentrations of 2.5, 3.5 and 6.5%. Suspensions were then cooled down to 5 °C and after 2 days of storage, the state of the solution was evaluated by turning the vial upside down followed by taking photographic images of the test tubes using a digital camera (PowerShot SD700 IS, Canon, Tokyo, Japan).

Statistical Analysis

Experiments were duplicated and all measurements were repeated three times. Means and standard deviations were calculated using Excel.

Results and Discussion

Influence of Holding Temperature on Gelation of SLN Suspensions

Gelation of Tween 20 stabilized SLN suspensions was initially observed visually after cooling. The suspensions were stable for a brief period after cooling but eventually formed a gel as can be seen in the photographic images of inverted test tubes containing SLN suspensions cooled to 5 °C and held for either 5 or 60 min (Fig. 1). Upon inversion of the test tubes, the samples stored for 5 min flowed into the bottom of the tubes, whereas those stored for 60 min remained at the top indicating gel formation.

To better understand the origin of this gelation phenomenon the phase behavior of bulk and emulsified tripalmitin was determined by DSC (Fig. 2). When bulk tripalmitin was heated from 30 to 75 °C, then cooled down to 10 °C, a number of thermal transitions were observed. Upon heating from 30 °C, three endothermic peaks were

Fig. 1 Picture of gel formation of SLN after cooling, on the left after holding for 5 min at 5 °C, on the right after holding for 60 min at 5 °C

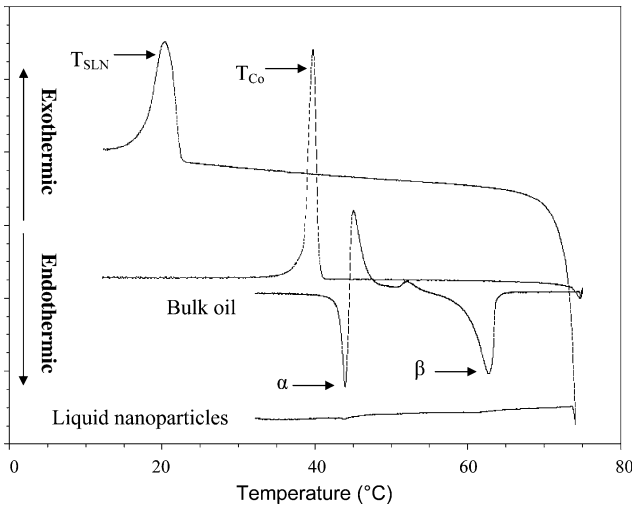

Fig. 2 Comparison of the DSC thermographs of bulk oil and liquid nanoparticles, heated from 37 °C at 10 °C/min to 75 °C then cooled down at 10 °C/min to 5 °C

observed at 45, 50 and 63 °C, which can be attributed to the melting of α, β' and β crystals, respectively. We can also see two exothermic peaks at 47 and 52 °C, which can be attributed to the $\alpha \rightarrow \beta'$ and $\beta' \rightarrow \beta$ polymorphic transformations, respectively [25]. Upon cooling from 75 °C, a single exothermic peak was observed at 37 °C, which can be attributed to the initial crystallization of the bulk tripalmitin into the α-polymorphic form [25]. These measurements are in good agreement with previous DSC measurements made on bulk tripalmitin [25].

A 10% (w/w) tripalmitin oil-in-water emulsion was prepared using the high-pressure homogenization method and kept at 37 °C. In this emulsions, no gelation was visually or microscopically observed in the nanoparticle suspensions during storage for two months. In addition, when this emulsion was heated in the DSC to 75 °C there was no melting sign or evidence of any phase transitions occurring, which suggested that the droplets had remained liquid at this storage temperature (Fig. 2). When the same emulsion was cooled from 75 °C in the DSC there was evidence of a single large exothermic peak at ~23 °C, which can be attributed to initial crystallization of the emulsified tripalmitin in the α-polymorphic form (T_C). Crystallization in the α-crystal form has also been observed with synchrotron X-ray scattering coupled with DSC under conditions comparable to those described in this paper [28]. The reason that the crystallization was observed at much lower temperatures for the emulsified tripalmitin than the bulk tripalmitin can be attributed to the effect of emulsification on the nucleation mechanism [29–34]. Nucleation in bulk oils is initiated by the presence of impurities that are evenly distributed throughout the oil. Once heterogeneous nucleation leads to crystal formation in one part of the oil, then it rapidly propagates throughout the whole volume of the oil. On the other hand, the oil in fine-disperse emulsions is divided into a very large number of droplets, so that the probability of finding an impurity in a particular droplet is extremely small [32, 35–39]. In addition, the droplets are effectively isolated from each other, so that crystallization in one droplet does not propagated to other droplets, hence the nucleation mechanism is usually different in bulk and emulsified oils. As a result, emulsified oil usually requires a lower temperature to promote nucleation and crystallization than bulk oil.

The DSC data indicate that the emulsified tripalmitin should be completely solid at 5 °C (Fig. 2). Nevertheless, the gelation of the SLN suspension held at 5 °C did not occur immediately, instead the solution remained fluid for some time before gelation was observed. The absence of any visible particulate structures in microscopic images of SLN suspensions immediately after cooling to 5 °C suggested that the samples were stable to particle aggregation (Fig. 3a). The small ($r < 150$ nm) SLN were below the detection limit of the optical microscope. Upon prolonged storage at 5 °C, large aggregated structures became visible in the suspension suggesting the formation of a network of crystallized SLN (Fig. 3b).

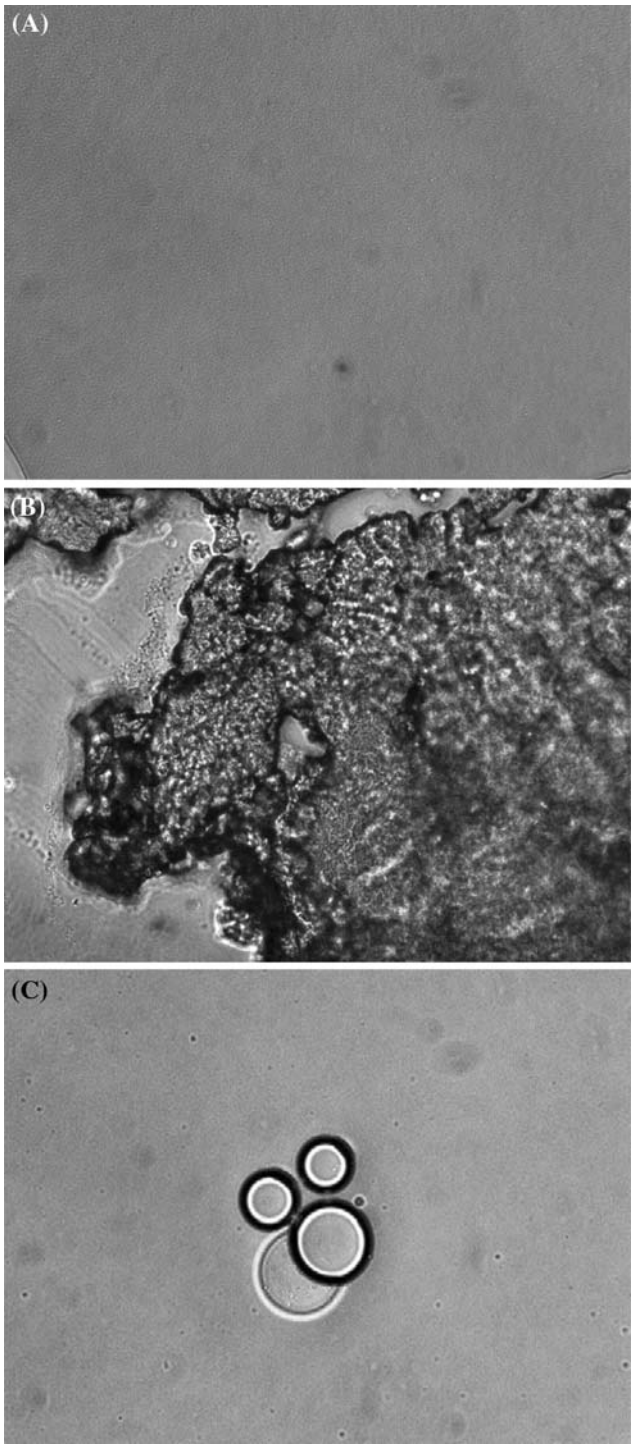

Fig. 3 Microscopic examination of SLN after crystallization and **a** held for after 5 min at 5°C, **b** held for 60 min at 5 °C and **c** after melting of the lipid phase at 75 °C. Magnification ×20

A more detailed examination of the gelation process was carried out using an oscillatory rheometer to measure G' and G'' as a function of holding time after SLN suspensions were cooled to different holding temperatures (1, 5, and 10 °C). The rheology data revealed that the kinetics of gel

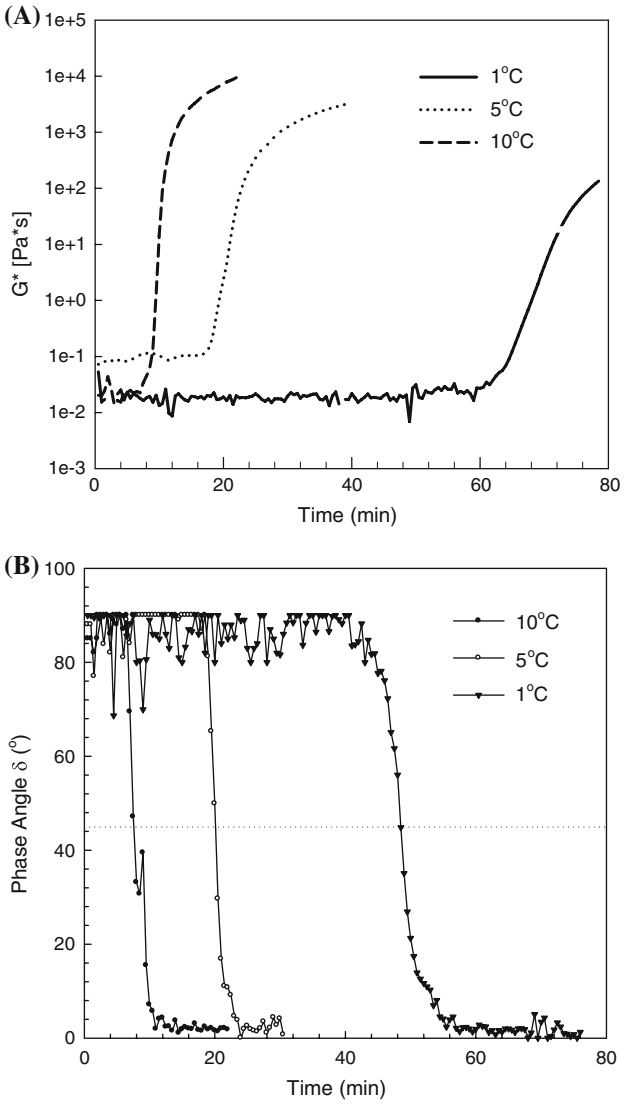

Fig. 4 **a** Complex modulus (G*) (*Y*-axis) as a function of SLN as a function of holding time (*X*-axis) at 1, 5 and 10 °C. **b** Phase angle (δ) (*Y*-axis) as a function of holding time (*X*-axis) at 1, 5 and 10 °C

network development was highly temperature sensitive i.e., the elastic modulus of SLN suspensions held at higher temperatures increased more rapidly than those held at lower temperatures (Fig. 4a). The apparent gelation time ($t_{\text{gel, app}}$) was defined as the time at which the loss and storage modulus became equal (i.e., phase angle = 45°). For samples held at 10, 5 and 1 °C, $t_{\text{gel, app}}$ was 10.1 ± 0.5, 23.2 ± 1.1 and 62.4 ± 4.2 min, respectively (Figs. 4b, 5). While gel formation slowed with decreasing temperature, all samples eventually gelled even at the lowest temperature tested.

Westesen and Siekmann [17] postulated after observation of crystallization events in lipid dispersions using Cryo-Transmission Electron Microscopy that suspensions may be destabilized due to morphological changes that

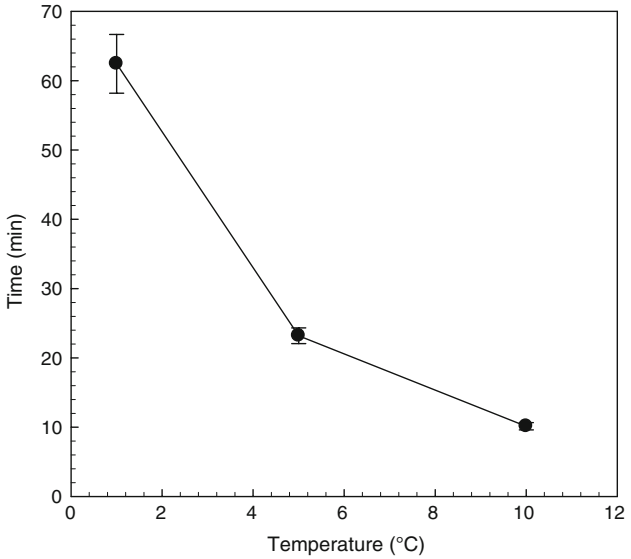

Fig. 5 Apparent gelation time (*Y*-axis) of Tween 20 stabilized tripalmitin SLN plotted versus holding temperature (*X*-axis)

occurred in the individual particles such as transformation of spherical to needle-shaped particles. The authors stated that this transformation is accompanied by an increase in contact area between the solvent and the lipid phase. They further postulated that surfactants required to cover and stabilize the newly created interfaces may not be able to diffuse rapidly enough to adsorb at the newly formed lipid–crystalline interfaces. Consequently, flocculation may be driven by the need to minimize the contact area of surfactant-free lipid crystals with the solvent. In addition, other authors suggested that the change of SLN from spherical to needle-shape was driven by the lipid matrix transforming from the α to β polymorphic structure [17, 21, 22, 40]. To further investigate whether similar processes may have occurred in our Tween-20 stabilized tripalmitin SLN, samples were examined by differential scanning calorimetry (DSC) and dynamic light scattering (DLS).

Investigation of Gelation Mechanism of Tween 20 Stabilized Tripalmitin SLN

DSC thermograms of tripalmitin emulsions subjected to a cooling–no holding–heating cycle showed evidence of two polymorphic forms of tripalmitin in SLN upon heating with endothermic transition peaks at 43–44 °C and 61–64 °C (Fig. 6a). These melting peaks agreed well with previously reported melting peaks observed in tripalmitin nanoparticles [20, 27], and correspond to the subcell arrangement of two polymorphic forms; the less ordered α-form with a hexagonal arrangement at 43–44 °C and the β-form with its highly ordered triclinic arrangement at 61–64 °C [25]. We did not observe the β′-form in our SLN. Since

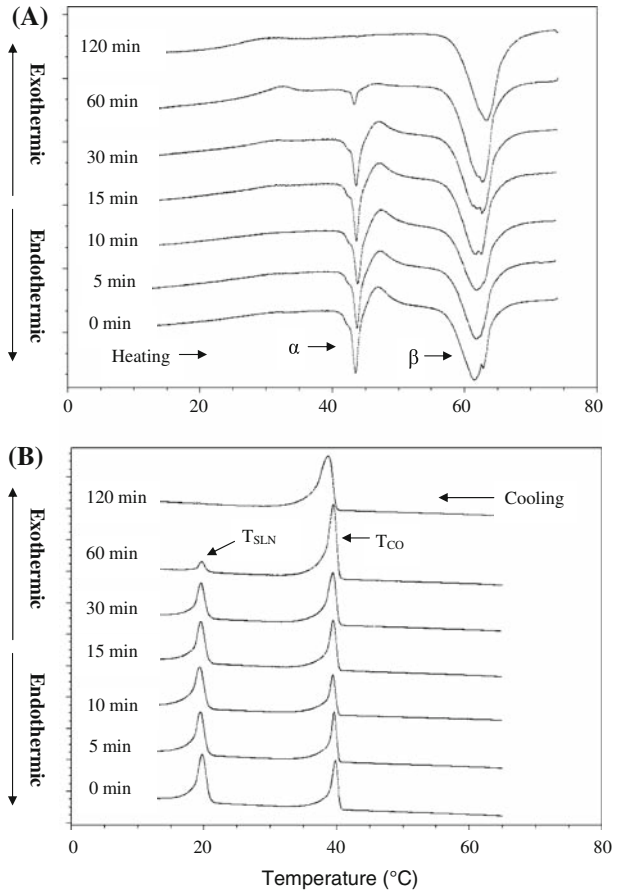

Fig. 6 **a** Heating enthalpy of tripalmitin SLN, kept at 37 °C, cooled to 1 °C at 5 °C/min (data not shown) and held for 0–120 min in the DSC, then heated at 10 °C/min to 75 °C. **b** Cooling enthalpy of tripalmitin SLN from 75 °C at 10 °C/min after crystallizing and melting shown in **a**

polymorphic transitions typically occur from α to β′ to β, it is likely that the formation and disappearance of the β′-form was too rapid to be detected by the instrument. Rapid polymorphic transitions into the final β-form prior to detection of β′ structures have been reported previously [25].

When the original tripalmitin oil-in-water emulsion containing liquid droplets was cooled for the first time we only observed a single crystallization peak (T_C), as shown in Fig. 2. However, when an emulsion was cooled to form a SLN suspension, then warmed to melt the tripalmitin, and then cooled again we observed two crystallization peaks (Fig. 6b). The first crystallization peak during the second cooling step was at 39.5 ± 0.2 °C and corresponds to the crystallization of bulk lipid (Fig. 2). This suggests that tripalmitin droplets may have coalesced upon melting of gelled SLN suspensions [41–43). Indeed, the presence of large coalesced lipid droplets after melting of gelled SLN suspensions was confirmed by optical microscopy (Fig. 3c). Similarly, a visible oil layer was formed on the

top of the test tube that contained melted, previously gelled SLNs (data not shown). The aggregated solid-lipid particles seen in Fig. 3b that form upon storage of the SLN dispersions for a prolonged period appear to coalesce into larger droplets after the samples are melted. Accordingly, the first crystallization peak was denoted as the coalescence peak (T_{CO}). The second peak (T_{SLN}) observed during the second cooling step was at 19.5 ± 0.2 °C and corresponds to the crystallization of SLN (ΔH_{SLN}). As mentioned earlier, the lipids inside small oil droplets crystallize at a much lower temperature than those within a bulk fat because of supercooling effects associated with differences in the nucleation mechanism [26, 37, 44]. Based on the above data, we therefore conclude that coalescence of particles after melting is a strong indication that gelation may have previously occurred and highlights the severity of the phenomenon i.e., aggregation and network formation in SLN suspensions can lead to destabilization of the suspension upon temperature increases. It should be noted that destabilization does not occur if the particles are never crystallized, i.e., if the warm tripalmitin emulsions are not cooled (Fig. 1). For example, when the warm tripalmitin emulsions were stored for 6 weeks at 37 °C without cooling, no significant particle size increase was observed. The mean particle radius was 146.5 ± 0.9 nm at day 0 and 148.0 ± 0.8 nm after 6 weeks.

DSC thermograms of tripalmitin SLN suspensions stored at different holding temperatures show that the enthalpy of melting of the α-form (ΔH_α) decreased with increasing storage time, with ΔH_α decreasing to zero (i.e., no peak) after 120 min at 1 °C, 30 min at 5 °C, and 10 min at 10 °C (Figs. 6a, 7a, 8a, 9a). This data indicates that the $\alpha \rightarrow \beta$ (polymorphic transformation occurred more rapidly at higher storage temperatures. Similarly, the crystallization enthalpy of supercooled lipid at 19.5 ± 0.2 °C (ΔH_{SLN}) decreased with increasing storage time and temperature (Figs. 6b, 7b, 8b, 9b), which suggests that the fraction of tripalmitin particles that had not aggregated decreased. When $\Delta H_{SLN}/\Delta H_C$ and $\Delta H\alpha/\Delta H_f$ (%) were plotted together and fitted to a linear regression model, a regression factor R^2 of 0.9887 for 1 °C, 0.9985 for 5 °C and 0.9980 for 10 °C was found (Fig. 10, data for 5 and 10 °C not shown) suggesting that the decrease in ΔH_{SLN} is directly related to the decrease in ΔH_α. Since a decrease in ΔH_{SLN} means that the particles are coalescing and crystallizing as large droplets or bulk oil, it is safe to assume that the polymorphic transformations from the α-form to the β-form are related to the destabilization of the SLN dispersion. Our results are therefore in agreement with previous studies that indicated that polymorphic transformations may be the basis for the destabilization mechanism of SLN suspensions [21, 40, 45].

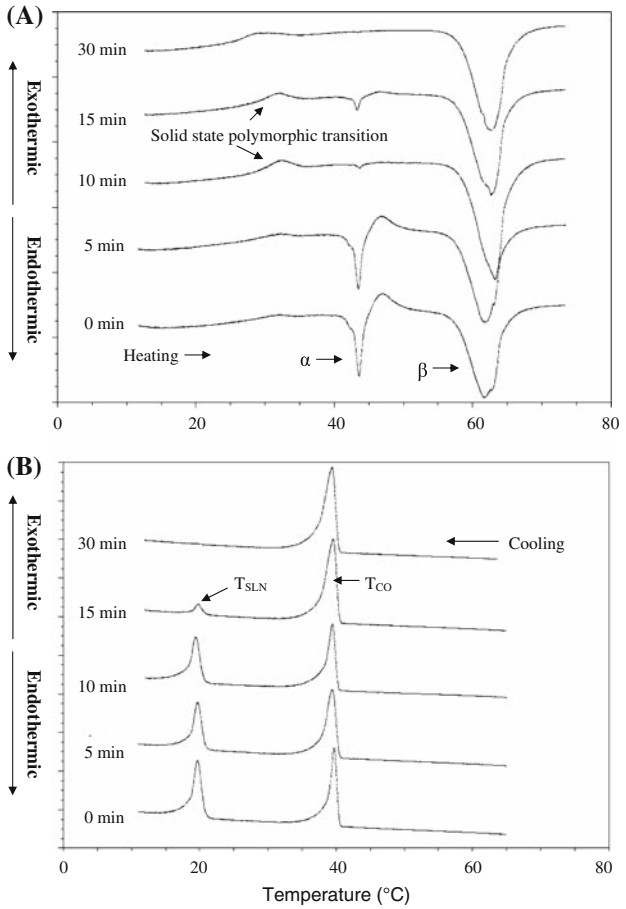

Fig. 7 **a** Heating enthalpy of tripalmitin SLN, kept at 37 °C, cooled to 5 °C at 5 °C/min (data not shown) and held for 0–30 min in the DSC, then heated at 10 °C/min to 75 °C. **b** Cooling enthalpy of tripalmitin SLN from 75 °C at 10 °C/min after crystallizing and melting shown in Fig. 7a

The relationship between the α-to-β polymorphic transformation of the lipid phase and the propensity for the SLN suspensions to gel was further highlighted by comparing the gelation time with the time taken for all of the α-from to disappear, $t_{\alpha \rightarrow \beta}$ (Fig. 11). There was a linear relationship between $t_{gel,\ app}$ and $t_{\alpha \rightarrow \beta}$, with a regression factor (R^2) of 0.999, which again strongly suggests that there is a direct relationship between the gelation process and the polymorphic transformation of the lipid phase.

Based on a recently published study by Bunjes et al. [22], we propose that SLN gelation occurs because of morphological changes in the lipid particles that are driven by polymorphic transitions (Fig. 12). Bunjes et al reported that solidified triacylglycerol nanoparticles were spherical when the lipid was in the α-polymorphic form, but needle-like when the lipid was in the β-polymorphic form [22]. Upon melting, the needle-shaped β-crystals tend to

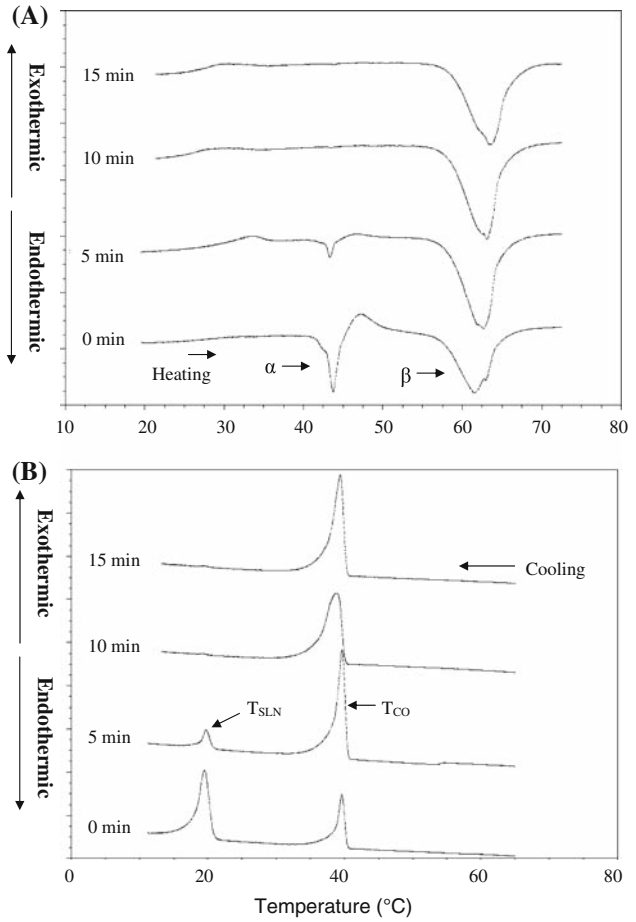

Fig. 8 **a** Heating enthalpy of tripalmitin SLN, kept at 37 °C, cooled to 10 °C at 5 °C/min (data not shown) and held for 0–15 min in the DSC, then heated at 10 °C/min to 75 °C. **b** Cooling enthalpy of tripalmitin SLN from 75 °C at 10 °C/min after crystallizing and melting shown in **a**

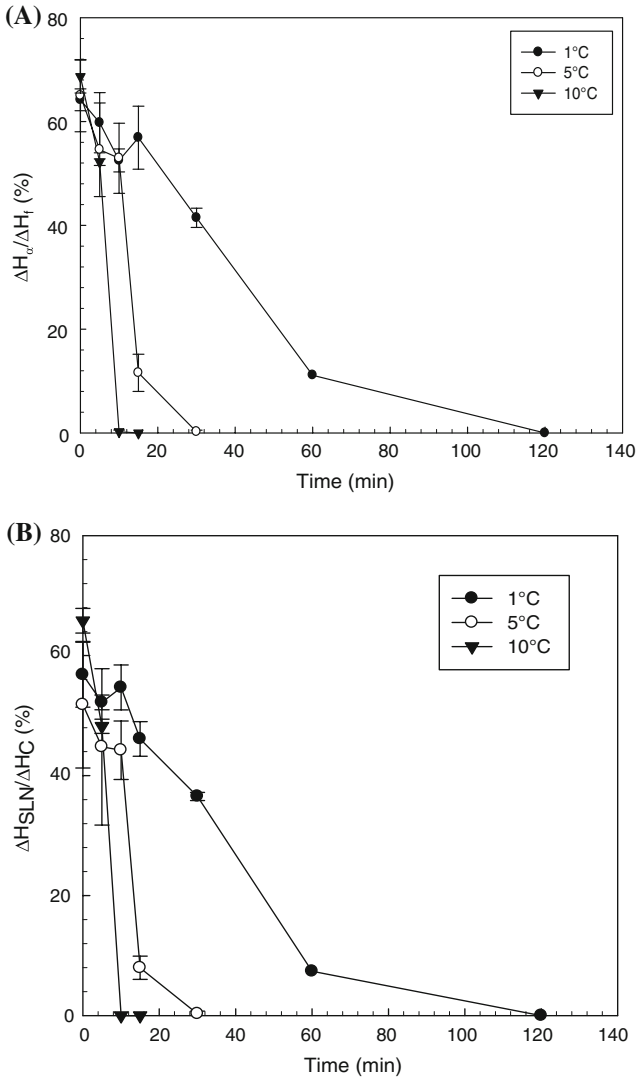

Fig. 9 **a** Enthalpy of α-crystals (Δ_α) divided by the specific heat of fusion for α-crystals ($H\Delta_f = 103$ kJ/mol) (49) of SLN as a function of holding time. **b** Enthalpy of supercooled crystallization peak (Δ_{SLN}) divided by overall enthalpy of crystallization of SLN (Δ_c) as a function of holding time

coalesce and upon re-cooling crystallize similarly to the bulk lipid at a higher temperature accounting for the observed increased crystallization enthalpy at 39 °C and the decreased ΔH_{SLN}.

Evolution of SLN Hydrodynamic Radius During Storage

Further insights into possible transitions from spherical to needle-shaped particles due to polymorphic transitions can be obtained using dynamic light scattering. Dynamic light scattering determines the hydrodynamic radius of a particle based on its Brownian motion in solution [46]. The hydrodynamic radius of needle-shaped particles is greater than that of spherical particles of the same mass [47]. For example, surface areas have been estimated to double upon conversion from spherical to cylindrical [1, 17]. Thus, polymorphic transformations that induce a change from spherical to needle-shaped particles should increase the hydrodynamic radius of SLN [48]. The hydrodynamic radius of liquid lipid droplets in emulsions maintained at 37 °C was determined to be 146.6 ± 0.8 nm with a polydispersity of 0.07 ± 0.015 nm (Fig. 13).

When the tripalmitin emulsions were held at 5 and 10 °C the hydrodynamic radius progressively increased with time, with the increase being more rapid at the higher temperature (Fig. 13). In addition, the particle size distribution remained monomodal during this period. This data may indicate that the particles were transforming from spherical to needle-shaped during the initial incubation period. However, after a certain time the particle size distribution became bimodal with a population of particles around 140 nm in size corresponding to the initial particles

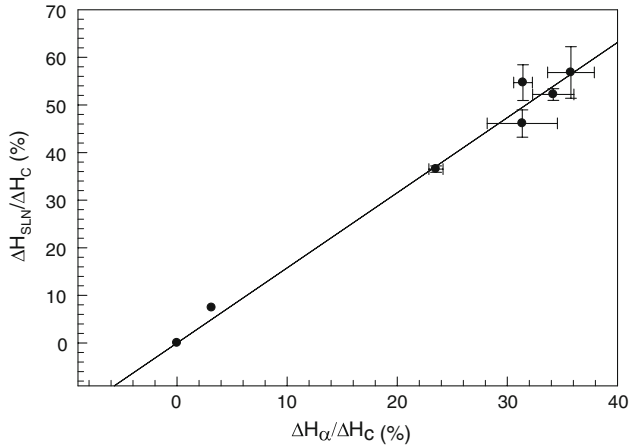

Fig. 10 Plot and linear regression of $\%\Delta H_\alpha/\Delta H_f$ (x-axis) versus $\Delta H_{SLN}/\Delta H_C$ (%) (y-axis)

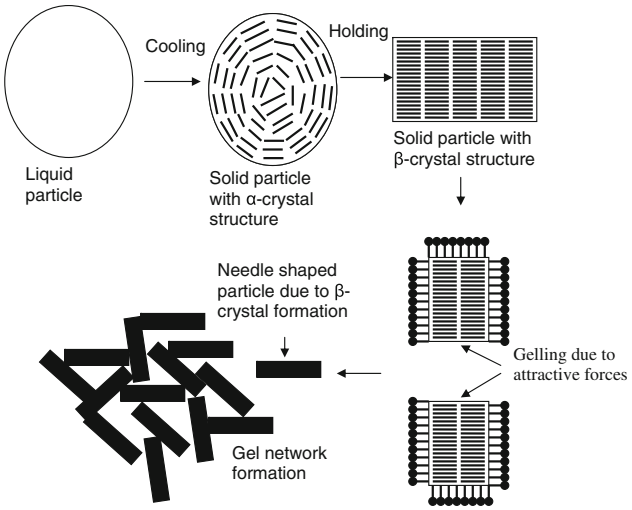

Fig. 12 Schematic drawing of the gelation mechanism; suggested structures of α-crystallized droplet based on electron microscope data (22)

and another population around 4 μm indicating the formation of large aggregates. Since the sample was diluted to prevent multiple scattering and particle–particle interactions, the timescale of the aggregation observed in the dilute solutions may not correspond to the onset of gelation observed in the rheometer, but the shape transformations should occur at the same rate since particles should change their shapes independently of their aggregation. The data suggests that there is indeed some degree of transformation from spherical to non-spherical in the initial stages of storage, which supports the assumption that the instability mechanism is driven by transformation of the droplet shape. An interesting observation is that initially, the solid particles appear to be smaller than the liquid oil droplets due to the fact that the density of crystalline lipid higher than that of liquid droplet (Fig. 13). Therefore crystallization of the particle may initially result in a size reduction but over time the hydrodynamic radius of the particles increased due to the shape transformation, eventually resulting in particles that are larger than the liquid particle. If the particles initially remained spherical when the liquid droplets crystallized into the α-polymorphic crystalline form, then one would expect the radius of the solid particles (r_S) to be slightly less than the radius of the liquid particles (r_L) because the solid state density (ρ_S) is greater than the liquid state density (ρ_L): $r_S = r_L \times \sqrt[3]{\rho_L/\rho_S}$. For the system used in this study, the densities of the solid and

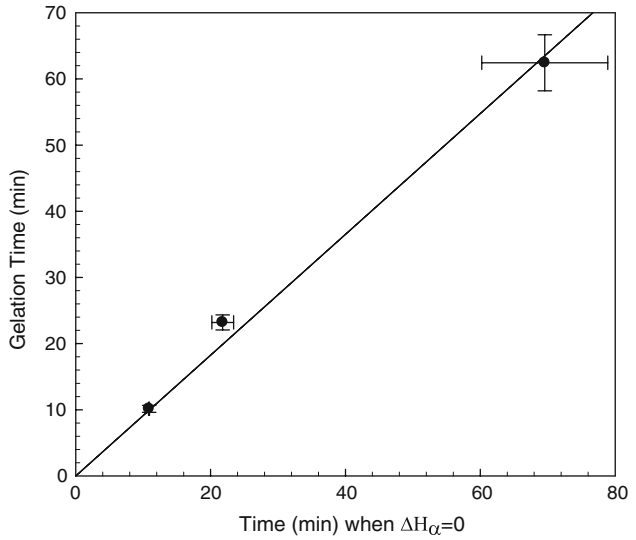

Fig. 11 Plot and linear regression of holding time when $\Delta H_\alpha/\Delta H_f = 0$ (from DSC thermograms) versus time of gelation (observed in the rheometer); $R^2 = 0.9993$

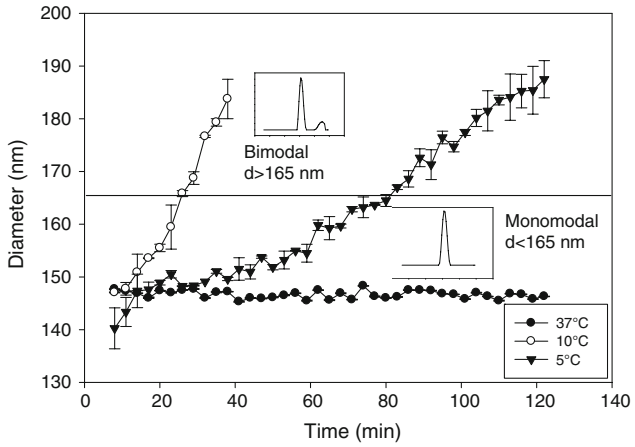

Fig. 13 Particle size distribution of SLN held at 5, 20 and 37 °C as a function of holding time measured with a dynamic light scattering technique

liquid phases are 1,010 (α-crystal) and 900 kg m^{-3}, respectively [49], hence one would expect the hydrodynamic radius of spherical solid particles to be about 141 nm compared to 146 nm for solid particle. This value is close to the value found by extrapolating the hydrodynamic radius versus time data for the emulsions held at 5 and 10 °C (see below). This would suggest that the particles formed in the SLN suspensions were initially spherical in shape.

The physicochemical mechanism proposed above to account for the observed gelation of the SLN suspensions is based on the assumption that the solid particles aggregate after the lipid phase has undergone a transformation from the α to β polymorphic form. This transformation of the molecular packing leads to a change in the overall morphology of the lipid particles that increases their total surface area, thus exposing non-polar lipid surfaces to water. Non-polar surfaces that are uncoated by surfactant tend to aggregate together through hydrophobic attractions to reduce the unfavorable contact between oil and water. To confirm this mechanism we examined the impact of adding additional surfactant to the aqueous phase of the emulsions prior to crystallization of the lipid phase but after the homogenization thus maintaining the droplet size while providing additional surfactant that can interact with the newly formed surfaces. The droplet size was also measured before and after addition of Tween 20 and no change was found (data not shown). We hypothesize that the degree of droplet aggregation would decrease in the presence of additional surfactant because there would be more available to cover any extra oil–water interface formed when the lipid particles change their shape. To test this hypothesis, various concentrations of Tween 20 buffer solutions (1, 2, 5% w/w) were added to the warm tripalmitin SLN suspension (37 °C) to obtain dispersions containing overall surfactant concentrations of 2.5, 3.5 and 6.5% (w/w). The suspensions with excess surfactant were then cooled down to 5 °C to crystallize the lipid. Emulsions containing no additional Tween 20 formed a gel as reported previously, but the emulsions containing an additional 1–5 wt% Tween 20 remained fluid-like, i.e., inversion of the test tube of the SLN suspension were Tween was added led to the samples flowing into the bottom of the tubes as shown in Fig. 1. This further supports the theory that new surfaces are formed after crystallization of the lipid, since addition of extra surfactant stabilizes the solution again after cooling.

This study has shown that tripalmitin SLN stabilized by Tween 20, a commonly used non-ionic surfactant in the food industry, are prone to particle aggregation and gelation. The proposed physicochemical origin of this instability is the polymorphic transition of the lipid phase from the α to β form during storage, which causes the solid nanoparticles to change from a spherical to a needle-like shape. The resulting increase in the surface area of lipid phase can lead to particle aggregation if there is insufficient surfactant present to cover it. There are a number of possible means to improve the stability of SLN suspensions based on these findings: (1) use a lipid source that prevents or retards the α to β polymorphic transition; (2) add enough surfactant to completely cover the lipid particle surfaces in both the liquid and solid states; (3) use a surfactant that prevents particle aggregation by increasing the repulsion between them and (4) use of high-melting emulsifier additives as templates to modify polymorphic crystallization avoiding the crystallization to reduce the impact of polymorphic transition on the droplet interface transition-induced gelation process. SLN are clearly promising new delivery systems that may help the food industry to create new functional foods, but more research using food-grade materials is required to control the microstructure of the particles to maximize stability and functionality.

Acknowledgments This work was supported by USDA CSREES hatch grants (MAS 0911 and MAS 831) and grants by the USDA National Research Initiative Programs (Award Number 2005-01357). Additional financial support was provided by the Leifur Eiriksson Foundation, Hrafnkellssjodur and Rannsoknarnamsjodur all located in Reykjavik, Iceland.

References

1. Westesen K, Bunjes H, Koch MHJ (1997) Physicochemical characterization of lipid nanoparticles and evaluation of their drug loading capacity and sustained release potential. J Control Release 48:223–236
2. Radomska-Soukharev A, Muller RH (2006) Chemical stability of lipid excipients in SLN-production of test formulations, characterization and short-term stability. Pharmazie 61:425–430
3. Schubert MA, Muller-Goymann CC (2005) Characterization of surface-modified solid lipid nanoparticles (SLN): influence of lecithin and nonionic emulsifier. Euro J Pharm Biopharm 61: 77–86
4. Jenning V, Thunemann AF, Gohla SH (2000) Characterization of a novel solid lipid nanoparticle carrier system based on binary mixtures of liquid and solid lipids. Int J Pharm 199:167–177
5. Muller RH, Mader K, Gohla S (2000) Solid lipid nanoparticles (SLN) for controlled drug delivery—a review of the state of the art. Euro J Pharm Biopharm 50:161–177
6. Muller RH, Weyhers H, zurMuhlen A, Dingler A, Mehnert W (1997) Solid lipid nanoparticles—a novel carrier system for cosmetics and pharmaceutics .1. Properties, production and scaling up Pharm Indus 59:423–427
7. Yang SC, Zhu JB, Lu Y, Liang BW, Yang CZ (1999) Body distribution of camptothecin solid lipid nanoparticles after oral administration. Pharm Res 16:751–757
8. zur Muhlen A, Schwarz C, Mehnert W (1998) Solid lipid nanoparticles (SLN) for controlled drug delivery—drug release and release mechanism. Euro J Pharm Biopharm 45:149–155
9. Yang Y, Feng JF, Zhang H, Luo JY (2006) Optimization preparation of chansu-loaded solid lipid nanoparticles by central

composite design and response surface method. Zhongguo Zhong Yao Za Zhi 31:650–653
10. Zhang LK, Hou SX, Mao SJ, Wei DP, Song XR, Lu Y (2004) Uptake of folate-conjugated albumin nanoparticles to the SKOV3 cells. Int J Pharm 287:155–162
11. Sivaramakrishnan R, Nakamura C, Mehnert W, Korting HC, Kramer KD, Schafer-Korting M (2004) Glucocorticoid entrapment into lipid carriers—characterization by parelectric spectroscopy and influence on dermal uptake. J Control Release 97:493–502
12. Videira MA, Botelho MF, Santos AC, Gouveia LF, de Lima JJ, Almeida AJ (2002) Lymphatic uptake of pulmonary delivered radio-labeled solid lipid nanoparticles. J Drug Target 10:607–613
13. Wang Y, Wu W (2006) In situ evading of phagocytic uptake of stealth solid lipid nanoparticles by mouse peritoneal macrophages. Drug Delivery 13:189–192
14. Muller RH, Keck CM (2004) Challenges and solutions for the delivery of biotech drugs—a review of drug nanocrystal technology and lipid nanoparticles. J Biotechnol 113:151–170
15. Wissing SA, Kayser O, Muller RH (2004) Solid lipid nanoparticles for parenteral drug delivery. Adv Drug Delivery Rev 56:1257–1272
16. Ahlin P, Kristl J, Smid-Korbar J (1998) Optimization of procedure parameters and physical stability of solid lipid nanoparticles in dispersions. Acta Pharm 48:259–267
17. Westesen K, Siekmann B (1997) Investigation of the gel formation of phospholipid-stabilized solid lipid nanoparticles. Int J Pharm 151:35–45
18. Westesen K, Siekmann B, Koch MHJ (1993) Investigations on the physical state of lipid nanoparticles by synchrotron-radiation X-ray-diffraction. Int J Pharm 93:189–199
19. Bunjes H, Koch MH, Westesen K (2003) Influence of emulsifiers on the crystallization of solid lipid nanoparticles. J Pharm Sci 92:1509–1520
20. Siekmann B, Westesen K (1994) Thermoanalysis of the recrystallization process of the melt-homogenized glyceride nanoparticle. Colloids surf 3:159–175
21. Jenning V, Schafer-Korting M, Gohla S (2000) Vitamin A-loaded solid lipid nanoparticles for topical use drug release properties. J Control Release 66:115–126
22. Bunjes H, Steiniger F, Richter W (2007) Visualizing the structure of triglyceride nanoparticles in different crystal modifications. Langmuir 23:4005–4011
23. Sato K, Garti N (1988) Crystallization and polymorphic transformation: an introduction. In: Sato K, Garti N (eds) Crystallization and polymorphism of fats and fatty acids. Marcel Dekker, New York, pp 3–7
24. Sato K, Ueno S, Yano J (1999) Molecular interactions and kinetic properties of fats. Progress Lipid Res 38:91–116
25. Himawan C, Starov VM, Stapley AGF (2006) Thermodynamic and kinetic aspects of fat crystallization. Adv Colloid Interface Sci 122:3–33
26. McClements DJ (1999) Food emulsions: principles, practice, and techniques. CRC Press, Boca Raton
27. Bunjes H, Koch MH (2005) Saturated phospholipids promote crystallization but slow down polymorphic transitions in triglyceride nanoparticles. J Control Release 107:229–243
28. Sonoda T, Takata Y, Ueno S, Sato K (2006) Effects of emulsifiers on crystallization behavior of lipid crystals in nanometer-size oil-in-water emulsion droplets. Crystal Growth Des 6:306–312
29. Kloek W, Walstra P, van Vliet T (2000) Nucleation kinetics of emulsified triglyceride mixtures. J Am Oil Chem Soc 77:643–652
30. Awad TS, Hamada Y, Sato K (2001) Effects of addition of diacylglycerols on fat crystallization in oil-in-water emulsion. Euro J Lipid Sci Technol 103:735–741
31. Awad TS, Sato K (2001) Effects of hydrophobic emulsifier additives on crystallization behavior of palm mid fraction in oil-in-water emulsion. J Am Oil Chem Soc 78:837–842
32. Awad TS, Sato K (2002) Fat crystallization in O/W emulsions controlled by hydrophobic emulsifier additives. In: Marangoni AG, Narine S (eds) Physical properties of lipids. Marcel Dekker, Inc., New York, pp 37–62
33. Awad TS, Sato K (2002) Acceleration of crystallization of palm kernel oil in oil-in-water emulsion by hydrophobic emulsifier additives. Colloids Surf B Biointerfaces 25:45–53
34. Walstra P (2003) Physical chemistry of foods. Marcel Decker, Inc., New York
35. Skoda W, Van den Tempel M (1963) Crystallization of emulsified triglycerides. J Colloid Sci 18:568–584
36. Mullin JW (1997) Crystallization. In: Mullin JW (ed) Crystallization. Butterworth Heinemann, Oxford, pp 172–292
37. Coupland JN (2002) Crystallization in emulsions. Curr Opin Colloid Interface Sci 7:445–450
38. Awad TS (2004) Ultrasonic studies of the crystallization behavior of two palm fats O/W emulsions and its modification. Food Res Int 37:579–586
39. Povey MJW, Awad TS, Hue R, Ding Y (2007) Crystallization in monodisperse emulsions with particles in size range 20–200 nm. In: Dickinson E, Leser M (eds) Food colloids: self-assembly and material science. The Royal Society of Chemistry, Cambridge, pp 399–412
40. Hatziantoniou S, Deli G, Nikas Y, Demetzos C, Papaioannou GT (2007) Scanning electron microscopy study on nanoemulsions and solid lipid nanoparticles containing high amounts of ceramides. Micron 38:819–823
41. Ghosh S, Peterson DG, Coupland JN (2006) Effects of droplet crystallization and melting on the aroma release properties of a model oil-in-water emulsion. J Agricult Food Chem 54:1829–1837
42. Thanasukarn P, Pongsawatmanit R, McClements DJ (2004) Impact of fat and water crystallization on the stability of hydrogenated palm oil-in-water emulsions stabilized by whey protein isolate. Colloids Surf A Physicochem Eng Aspects 246:49–59
43. Thanasukarn P, Pongsawatmanit R, McClements DJ (2004) Influence of emulsifier type on freeze–thaw stability of hydrogenated palm oil-in-water emulsions. Food Hydrocolloids 18:1033–1043
44. Gulseren I, Coupland JN (2007) The effect of emulsifier type and droplet size on phase transitions in emulsified even-numbered n-alkanes. J Am Oil Chem Soc 84:621–629
45. Freitas C, Muller RH (1999) Correlation between long-term stability of solid lipid nanoparticles (SLN (TM)) and crystallinity of the lipid phase. Euro J Pharm Biopharm 47:125–132
46. Jores K, Mehnert W, Drechsler M, Bunjes H, Johann C, Mader K (2004) Investigations on the structure of solid lipid nanoparticles (SLN) and oil-loaded solid lipid nanoparticles by photon correlation spectroscopy, field-flow fractionation and transmission electron microscopy. J Control Release 95:217–227
47. Mehnert W, Mader K (2001) Solid lipid nanoparticles—production, characterization and applications. Adv Drug Delivery Rev 47:165–196
48. Bunjes H, Westesen K, Koch MHJ (1996) Crystallization tendency and polymorphic transitions in triglyceride nanoparticles. Int J Pharm 129:159–173
49. Hagemann JW (1988) Thermal behavior, polymorphism of acylglycerides. In: Sato K, Garti N (eds) Crystallization and polymorphism of fats and fatty acids. Marcel Dekker, New York